JOURNAL OF SOLID STATE CHEMISTRY 96, 247–257 (1992)

# Ionically Conductive Chalcogenide Glasses

ANNIE PRADEL AND MICHEL RIBES

*Laboratoire de Physicochimie des Matériaux Solides, U.R.A. D0407 CP003, Université de Montpellier II, Sciences et Techniques du Languedoc, Place E. Bataillon, 34095 Montpellier Cedex 05, France*

Received July 12, 1991

A satisfactory understanding of ionic transport mechanisms in glasses has not been achieved to date. Recently, models (coupling model, jump diffusion model, and diffusion controlled relaxation model) based on study of the dynamic of the mobile ions have been developed. To date they have been mainly supported by data obtained on poorly conductive glasses. The very recent results obtained on highly conductive glasses in the systems $Ag_2X$–$GeX_2$–(AgI) ($X$ = S, Se) and $Li_2S$–$SiS_2$–(LiI) in a very large frequency domain by mechanical, electrical, NMR spectroscopies, and by QENS are used to illustrate these models. Also, structural effects influencing the dc conductivity in these glasses are presented and interpreted in terms of the weak electrolyte theory and the Stuart–Anderson approach. 

## Introduction

Considerable research effort over the past 20 years has concerned the family of materials, referred to as solid electrolytes, which comprises materials with reduced structural organization such as glasses.

Until recently the main aim of work on ionic conductive glasses was to seek increasingly high conductivity. For example, progress was made in a period of a few years from mediocre $Li^+$ conductivity of some $10^{-9}\,Sm^{-1}$ to high conductivity of some $10^{-1}\,Sm^{-1}$ at ambient temperature. Today there is less stress on this effort to minimize the ohmic drop caused by the electrolyte in electrochemical devices. Indeed, conductivity is no longer the limiting factor, since applications are envisaged in microionics—the most promising field for glasses. The use of thin films minimizes the internal resistance of the devices and hence allows much lower conductivities while keeping ohmic drop to reasonable proportions.

On the other hand, transport phenomena in glasses are still not well known. Although the predictive nature of some thermodynamic approaches such as the weak electrolyte theory (*1*) enable the synthesis of high-performance materials, they do not allow the microscopic modelling of ion movements. The first attempt was made forty years ago, when Anderson and Stuart related the activation energy of conduction to several characteristic parameters of the glasses (*2*).

The two preceding models are based essentially on measurements of $\sigma_{dc}$ and do not attempt to explain the frequency responses of ionic conductive glasses. It appeared only recently that such investigations should provide information on the dynamics (relax-



0022-4596/92 $3.00

ational aspect) of mobile species in noncrystalline solids such as glasses.

Three models have been proposed to date. They are the Coupling Model developed by Ngai and co-workers (*3–5*), the Jump Diffusion Model developed by Funke and co-workers (*6, 7*) and the Diffusion Controlled Relaxation Model from Elliot and coworkers (*8–10*). They first attempted to account for the frequency-dependence of conductivity, which is a consequence of the nonexponential nature of the relaxation in the time domain. They have then been extended to NMR measurements and attempt in particular to explain the departure from the classic BPP model describing the temperature dependence of the spin lattic relaxation rate (SLR) (*11–13*).

As is admitted by the authors themselves, these models are based on experimental data for conventional oxide glasses, which are generally poor conductors. Study of chalcogenide glasses, whose conductivity is extremely high in comparison to the oxide equivalents, could provide experimental data giving more information and thus more solid bases for the models above. In particular, correlations could be established between conductivity and NMR measurements, since the "high temperature" branch of the "log $(T_1)^{-1}$ vs $T^{-1}$" curves may be reached.

We attempted to illustrate this below with examples taken mainly from the lithium thiosilicate or silver thiogermanate families. We first examined the "structural" effects on conductivity: the role of chalcogens, dopants, and formers. Ion dynamic was then investigated. The various conditions of glass synthesis and general studies on their properties are not discussed. Interested readers will find this information in Refs. (*14*) to (*16*).

## Structural Effects

### *A. Role of Chalcogen ($X$ = O, S, Se): $Li_2X$–$SiX_2$ System*

The main data on these glasses are presented in Fig. 1. The sulphide and selenide

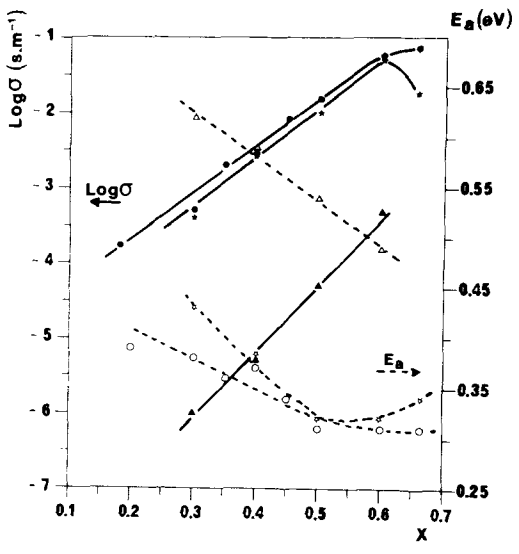


FIG. 1. Composition dependence of conductivity (25°C) and of activation energy in the systems $xLi_2X$–$(1-x)SiX_2$ ($X$ = O (▲), S (★), Se (●)).

glasses have comparable electrical characteristics; their conductivities and activation energies are identical to within the margin of experimental error. In contrast, the corresponding oxide glasses are distinctly different; conductivities are much lower and activation energies are higher (*17, 18*).

All these results lead to suggesting that the main factor which governs ion movement in these glasses is anion polarizability. This is comparable for sulphur (7.3) and selenium (7.5) and much lower for oxygen (3.1). This was forecast by the weak electrolyte theory, which claims that increasing $\sigma$ is the same as increasing the dielectric constant of the medium by acting on atomic polarizability (*1*).

The similar electrical behavior of sulphides and selenides, and the difference with oxides, also applies to the structural aspects. Indeed, oxide glasses consist only of $SiO_4$ tetrahedra sharing corners, whereas sulphide and selenide glasses contain tetrahedra with common edges. This was shown clearly by high resolution $^{29}Si$ NMR; this

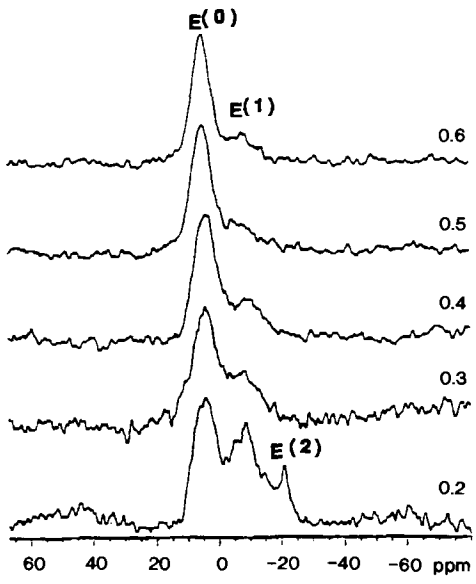


FIG. 2. 59.7 MHz $^{29}$Si MAS NMR spectra of glasses in the system $x$$Li_2S$–$(1 - x)SiS_2$. (Spinning speeds 4 to 4.5 kHz. Typical conditions: relaxation delay 40 min., 16 scans) (*21*).

technique is an extremely powerful tool for characterizing the short range order in glasses. Specifically, $^{29}$Si NMR chemical shifts discriminate between the various types of $SiO_4$ tetrahedra present in alkali silicate glasses. This is expressed by the $Q(n)$ nomenclature, where $n$ specifies the number of Si–O–Si bridges per silicon atom. The NMR spectra evolve continuously with an increasing alkali oxide modifier content $x$, making it possible to determine the relative amounts of the different $Q(n)$ species (*19, 20*). In lithium thiosilicate glasses (*21*), $^{29}$Si chemical shift differentiation arises not from the presence of non-bridging sulphur units (i.e., the various $Q(n)$ species) but from the presence of edge-sharing units (i.e., the various $E(n)$ species). The compositional evolution of the spectra (Fig. 2) is hence due to a shifting balance between corner- and edge-sharing silicon tetrahedra, as successive introduction of $Li_2S$ creates non-bridging sulphur atoms. Specific peak assignments are summarized in Fig. 3 in the form of a matrix that assigns a $Q(n)$ and an $E(n)$ symbol to each of the microstructures shown. The first results of MAS NMR studies on $Li_2Se$–$SiSe_2$ glasses confirm that they are structurally similar to their sulphur equivalents (*22*).

### *B. Dopant Effect: $Li_2S$–$SiS_2$–LiI System*

Dissolving a salt of the same cation as that responsible for conduction can be used to increase the conductivity of a glass. Thus, 0.6 $Li_2S$–0.4 $SiS_2$, the most conductive of the sulphur glasses, was doped with LiI (*16*). A slight improvement of conductivity with the lithium ion content was observed. Conductivity of the glass 0.7 (0.6 $Li_2S$–0.4 $SiS_2$) 0.3 LiI attained the peak values observed in $Li^+$ conductive sulphide glasses ($10^{-1}$ $Sm^{-1}$).

Structural study of these materials by Raman spectroscopy shows that the iodine is not inserted in the macromolecular chains but plays the role of plasticizer, enhancing the cooperative movement of the chains. This accounts for the decrease in $T_g$ during the dissolution of LiI ($\Delta T_g \approx 30$°C). Here again, the increase in the dielectric constant of the medium by the introduction of a highly polarisable ion (I) was probably an important factor in the increase in conductivity observed.

### *C. Stabilizer Effect: $Li_2S$–$SiS_2$–$Al_2S_3$ System*

The effects both on the structure of the material and on its electrical characteristics, related to the introduction of a "stabilizing" compound, were examined. Such a compound cannot itself behave as a network former, but it can become inserted in the macromolecular network in the presence of another former.

Raman spectroscopy (Fig. 4) showed that the introduction of $Al_2S_3$ in a 0.5 $Li_2S$–0.5 $SiS_2$ glass results in a decrease in non-bridging Si–S bonds and the appearance of aluminium at tetrahedral sites. These two fea-

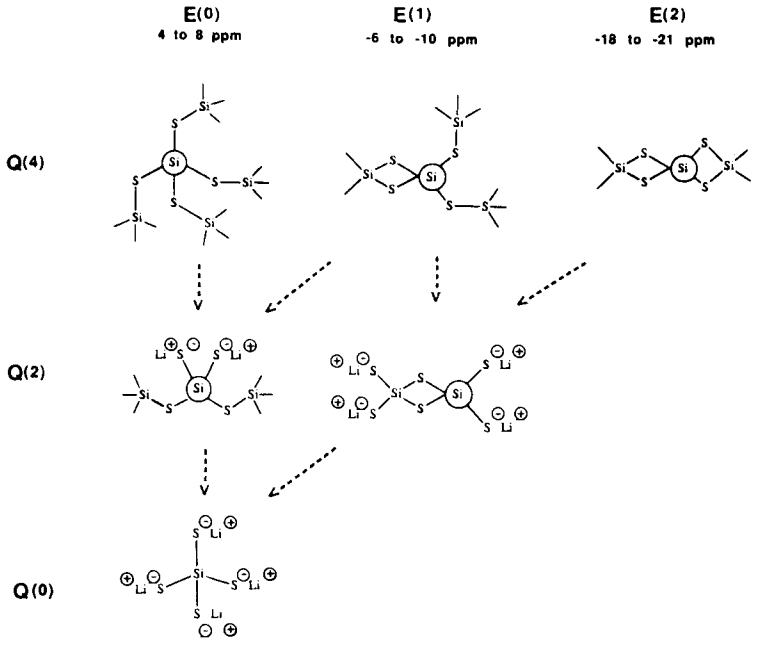


FIG. 3. Peak assignments to silicon microstructures in $Li_2S$–$SiS_2$ glasses. Each microstructure can be identified by both a $Q(n)$ and an $E(n)$ symbol. The arrows indicate the process of network conversion with increasing amount of $Li_2S$ (*21*).

tures confirm that Si is substituted by Al in the thiosilicate network as follows:

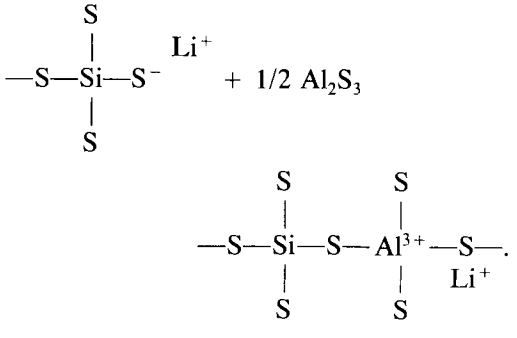

$Li^+$ thus plays a charge compensation role.

These results explain the increase of $T_g$ ($\Delta T_g \approx 80°C$), reflecting the steady decrease in the number of non-bridging sulphur atoms (*23*).

The replacement of half of the silica atoms by aluminium in the 0.5 $Li_2S$–0.5 $SiS_2$ glass results in a fall in conductivity from $10^{-2}$ to $3.5 \times 10^{-3}$ $Sm^{-1}$ and in a simultaneous increase in activation energy (from 0.32 to 0.39 eV).

These variations are justified by the structure proposed and Anderson–Stuart's model (*2*). In this model, the activation energy is the sum of two contributions; one is electrostatic ($E_b$) and shows the ionicity of the $M^+ \ldots\ldots X^-$ ($X$ = O, S, Se) bond, the other is elastic ($E_s$) and shows the elastic strain of the glass when the ion moves (movement through doorways). Although the growing number of lithium atoms playing a charge compensation role leads to considering that there is a slight decrease in the electrostatic part of activation energy, the strong increase in $T_g$ indicates an increase in the elastic part of this energy. This second effect is doubtless more important and

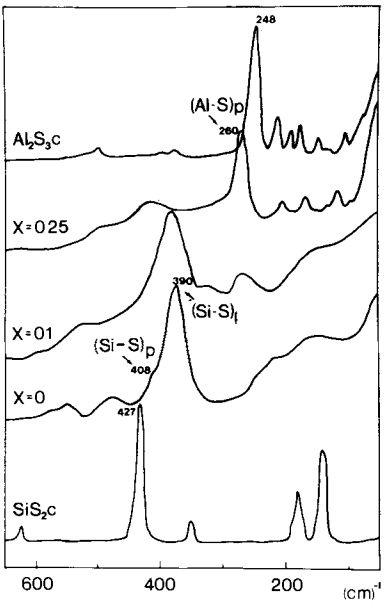


FIG. 4. Composition dependence of Raman spectra in 0.5 $Li_2S$–$xAl_2S_3$–$(0.5 - x)SiS_2$ glasses. p and I stand for bridging and non bridging sulphur, respectively.

makes it possible to understand the changes observed in electrical properties.

It is noted that these structural effects are small as they result in a decrease in conductivity by a factor of only 3.

### *D. Mixed Former Effect: $Li_2S$–$SiS_2$–$GeS_2$ System*

In some cases, oxide glasses containing two network formers possess better conductivity than their binary counterparts. It was interesting to find out whether such a mixed former effect could be observed in sulphide glasses and, if so, to attempt to relate the phenomenon to the structure of the materials. The $y$ $Li_2S$-$(1 - y)$ $[(1 - x)$ $SiS_2 - x$ $GeS_2]$ ($y$ = 0.3–0.5 and $0 < x < 1$) systems were studied. Two cases were considered, depending on the values of $y$:

—In the glasses richest in lithium, $y$ = 0.5, a monotonic variation of all the characteristic properties ($T_g$, $\rho$, $\sigma_{dc}$) and monotonic evolution of Raman spectra show that homogeneous substitution of silica by germanium took place in the glass matrix.

—In the glasses with the lowest lithium contents, $y$ = 0.3, all the characteristic properties display non-linear evolution (Fig. 5). An increase of two orders of magnitude of conductivity was observed with rates of replacement of silica by germanium of about 0.5. This corresponds to a sharp decrease in density, an increase in the $T_g$.

Raman spectroscopy showed that this mixed former effect is the result of a phase separation with the appearance of a phase with $Li_2SiS_3$ composition. This extremely conductive phase imposes its conductivity on the materials (*16, 24*). This shows the importance of knowledge of the "macroscopic" structure of the glasses in investigation of transport properties.

## Dynamic Studies

Several spectroscopic techniques using the greatest possible range of frequencies with the application of different stimuli were used to obtain information as complementary as possible: mechanical spectroscopy (several Hz), impedance spectroscopy (10–$10^7$ Hz), nuclear magnetic resonance ($10^7$–$10^8$ Hz), and quasi-elastic neutron scattering ($10^{10}$–$10^{11}$ Hz). The measurement procedures have been described previously (*25–29*).

### *A. Results*

Typical Arrhenius plots of the conductivities $\sigma'_{ac}$ at 4 different frequencies (10 kHz, 100 kHz, 1 MHz, 10 MHz), together with $\sigma_{dc}$, are shown in Figs. 6–8 for 0.5 $Ag_2S$–0.5 $GeS_2$ (Fig. 6), 0.2 $Ag_2Se$–0.8 $GeSe_3$ (Fig. 7), and 0.5 $Li_2S$ 0.5 $SiS_2$ (Fig. 8) glasses. Arrhenius plots of the SLR rate $T_1^{-1}$ have been included in the figures together with the values of parameter $S$. This parameter accounts for the power law dependence of the real part of the complex conductivity

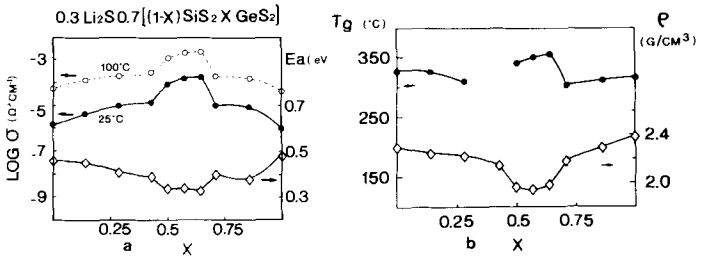


FIG. 5. Composition dependence of conductivity and activation energy (a) and of density and glass transition temperature (b) in 0.3 $Li_2S$ 0.7 [$(1 - x)SiS_2 - xGeS_2$] glasses (*16*).

$$\sigma'_{ac} = \sigma_{dc} + A\omega^s,$$

where $A$ is a temperature-dependent parameter and $0 < S < 1$.

The temperature dependence of SLR rate $T_1^{-1}$ at 2 frequencies 15.8 and 77.7 MHz for the $Li_2S$–$SiS_2$ glass system are shown in Fig. 9. An isochronal (1 Hz) measurement of complex mechanical modulus $g(\omega)$ is shown in Fig. 10 for the 0.2 $Ag_2Se$–0.8 $GeSe_3$ glass. QENS data for 0.5 $Ag_2S$–0.5 $GeS_2$ glass plotted as $S(Q)\ \Delta E$ vs $Q^2$, where $\Delta E$ is the HWHM of the QENS line shape, $S(Q)$ is the quasi-elastic Ag–Ag structure factor ob-

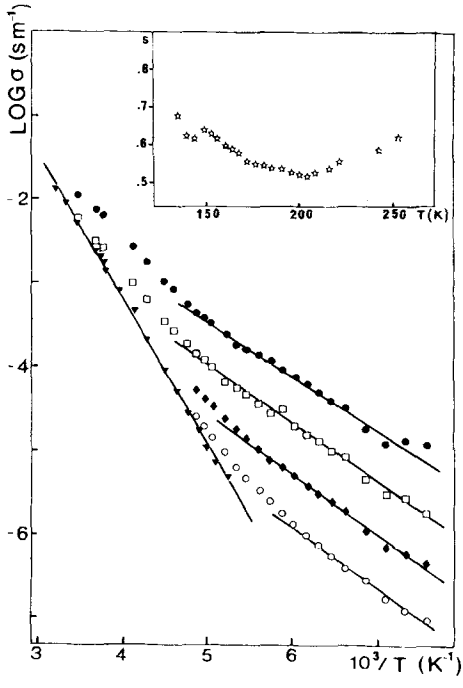


FIG. 6. Temperature dependence of $\sigma$ for 0.5 $Ag_2S$–0.5 $GeS_2$ glass. $\sigma_{dc}$ (▼), $\sigma_{ac}$ at 10 kHz (○), 100 kHz (◆), 1 MHz (□), 10 MHz (●) (*29*). Temperature dependence of $S$ is shown in the inset.

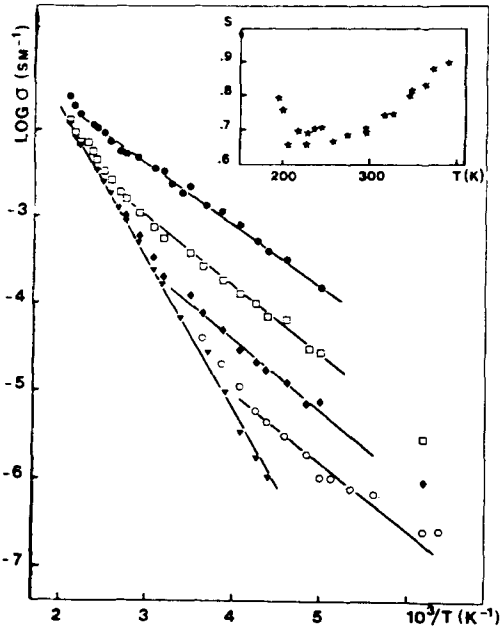


FIG. 7. Temperature dependence of $\sigma$ for 0.2 $Ag_2Se$–0.8 $GeSe_3$ glass (see Fig. 6 for symbols) (*27*). Temperature dependence of $S$ is shown in the inset.

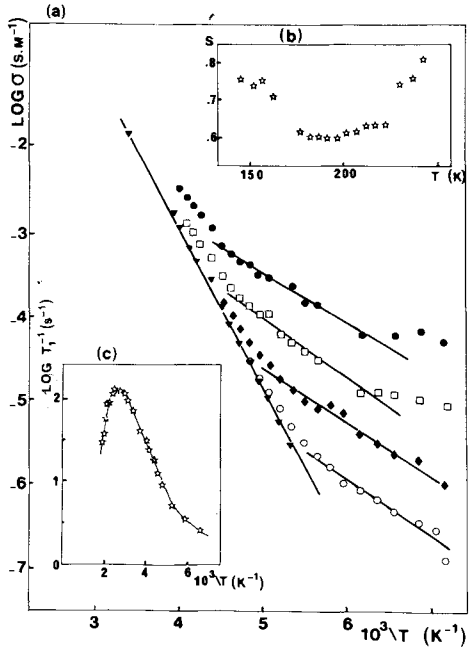


FIG. 8. Temperature dependence of $\sigma$ (a), $S$ (b), $T_1^{-1}$ at 15.8 MHz (c) for 0.5 $Li_2S$–0.5 $SiS_2$ glass (see Fig. 6 for symbols) (*28*).

tained approximately by summing over the QENS spectrum, $Q$ being the scattering factor, are shown in Fig. 11. Characteristic data for all the glasses studied are provided in Table I.

### *B. Discussion*

Measurements of $\sigma'_{ac}$ (*27–29*) at different frequencies for all the glasses studied give a group of practically parallel lines within a varied temperature range. It can be deduced that there is an activation energy $E'_{ac}$ which is practically independent of the frequency for a given system. It is much smaller than the activation energy $E_{dc}$ and makes it possible to determine a parameter $\beta = \langle E'_{ac}\rangle/E_{dc}$, which thus appears to be independent of frequency within the temperature range in question. This parameter $\beta$, introduced by Ngaï and co-workers (*3–5*) when developing the Coupling Model, corresponds to that of the empirical Kohlraush, Williams and Watts function:

$$\phi(t) = \exp[-(t/\tau)\beta] \quad 0 < \beta < 1.$$

The parameter $S$ (shown in Figs. 6–8) is temperature-dependent; the minimum is a more or less marked pseudo-plateau in a temperature range which appears to correspond to that of the linear portions of the "log $\sigma'_{ac}$ vs $T^{-1}$" curves. The temperature-dependence of $S$ had already been observed in oxide glasses (borate and germanate) (*30, 31*) but the pseudo-plateau was not detected. The temperature range of the studies was probably not broad enough. Parameters $S$ and $\beta$ are linked by the equation $S + \beta = 1$, as shown in Table I.

In NMR, although the simple BPP model can be criticized because it assumes a simple exponential for the correlation function $G(\tau)$, some of its predictions concerning the temperature-dependence of the SLR rate $T_1$ remain valid if a stretched exponential function is used. For example, the high temperature branch of the curve "log $T_1^{-1}$ vs $T^{-1}$" is frequency-independent whereas the low temperature branch is frequency-dependent. The activation energy of the high temperature branch would thus be expected to be equal to that of $\sigma_{dc}$ because this corresponds to the part of conductivity that is independent of the frequency. This was observed (Fig. 9 for $f$ = 15.8 MHz and Table I) (*25*). It should be noted that only the very high conductive sulphide glasses display this feature, which had hardly ever been observed in oxide glasses.

Excellent agreement was observed between activation energies $E'_{ac}$ and those ($E'_{NMR}$) deduced from the low temperature branches of the $T_1$ curves. It would appear that, like $E'_{ac}$, $E'_{NMR}$ is independent of the investigation frequency chosen (Larmor frequency in this case), at least for frequencies of less than 40 MHz, as has been shown recently by Martin and co-workers (*32*) in a study of the same type of glass (0.56

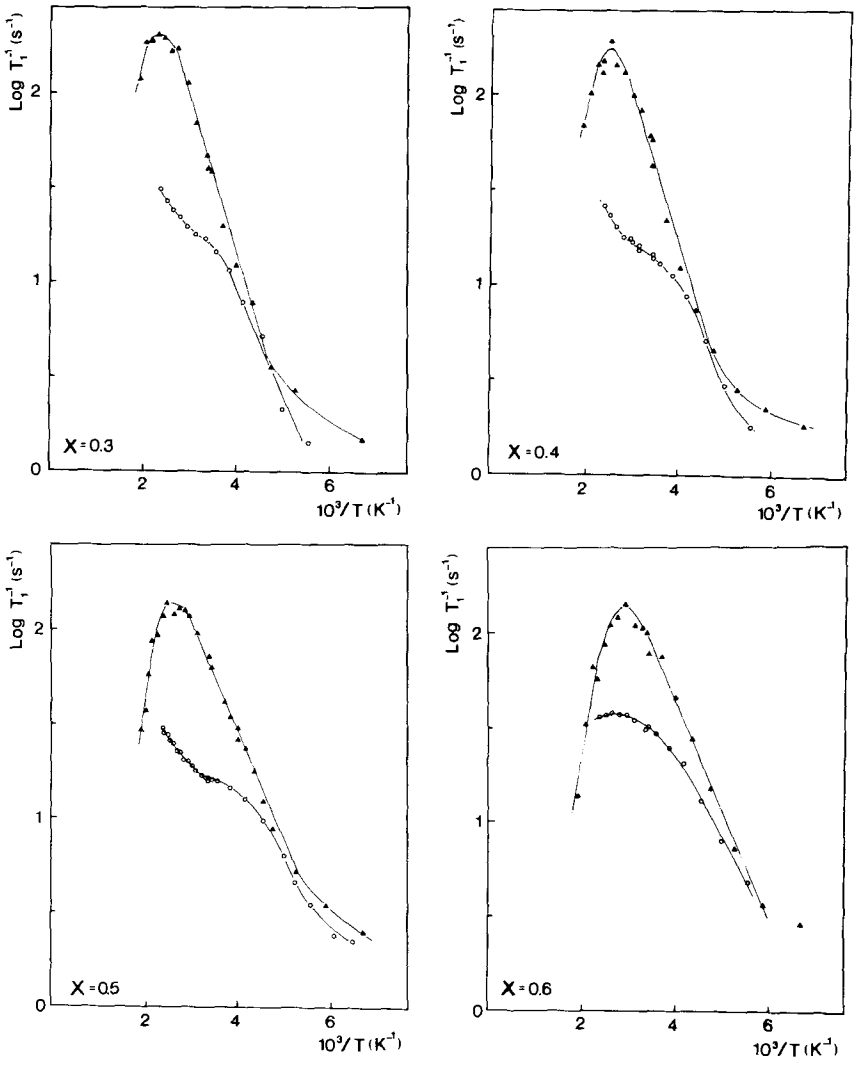


FIG. 9. Temperature dependence of $T_1^{-1}$ at 15.8 MHz (▲) and 77.7 MHz (○) for $x$$Li_2S$–$(1 - x)$$SiS_2$ glasses.

$Li_2S$–0.44 $SiS_2$) at four different frequencies (4, 7, 22, and 40 MHz). At lower temperatures, a weakly thermally activated process occurs. A two-level tunnelling model is often used to describe this "extra" relaxation (*13*, *33*). It is relevant that a comparable phenomenon appears to occur in $Li_2S$–$SiS_2$ glasses within the same temperature range on the conductivity curves.

All these analogies confirm that the process at the origin of the relaxation is the same whatever the applied stress, magnetic field in NMR and electrical field in $\sigma'_{ac}$ measurements.

In $x$$Li_2S$–$(1 - x)$ $SiS_2$ glasses, measurements of $T_1$ at a higher frequency (77.7 MHz) revealed more complex behavior of the low temperature branches. Indeed, a second

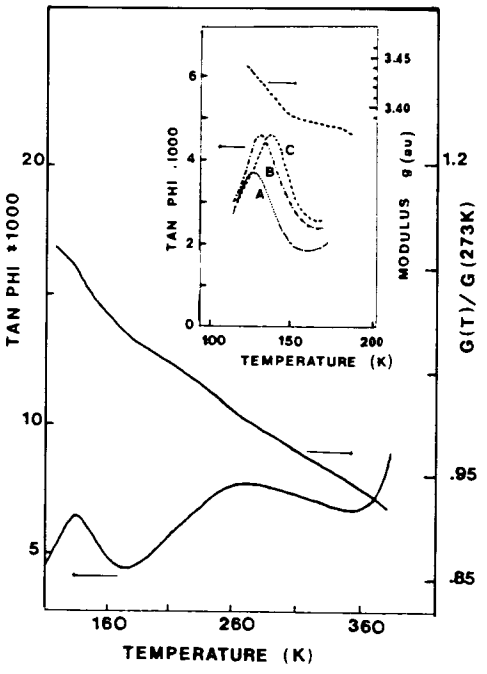


FIG. 10. Temperature dependence of isochronal (1 Hz) Tan Phi and modulus $G$ for 0.2 $Ag_2Se$–0.8 $GeSe_3$ glass. Inset shows the low temperature peak at 3 frequencies: 0.1 Hz (A), 0.3 Hz (B), and 1 Hz (C) (*27*).

event appeared on the $T_1$ curves as can be seen in Fig. 9. It is less marked for $x = 0.6$, but the considerable width of the peak reveals its presence. Comparable behavior has been shown in the $T_1$ curves of $Li_2S$–$B_2S_3$ glasses measured at a high frequency (117 MHz) (*34*). These features have not yet been explained. Might they be a second type of lithium relaxation? It would be particularly interesting to perform conductivity measurements in this frequency range to find out if the analogy between NMR and electrical measurement is confirmed.

Because of the problems involved in sample preparation (rectangular bars, 40 × 4 × 1 $mm^3$), mechanical spectroscopy measurements have been carried out to date only on 0.2 $Ag_2Se$–0.8 $GeSe_3$ glass (*27*). The first measurements were of the network former alone in order to distinguish between the relaxation phenomena related to the matrix and those related to mobile ions. In addition to the main $\alpha$ relaxation toward the vitreous transition temperature, a second relaxation peak $\beta$ attributed to the relaxation of the Se–Se–Se microdomains appeared at a lower temperature. The addition of $Ag_2Se$ modifier resulted in a third low temperature relaxation peak (Fig. 10) whose 0.3 eV activation energy was fully comparable to $E_{dc}$ (0.34 eV) in these glasses.

Quasi-elastic neutron scattering (QENS) measurements were performed on 0.5 $Ag_2S$–0.5 $GeS_2$ glasses (*29*, *35*). The diffusion coefficient $D_n$ of the $Ag^+$ ions was determined at different temperatures from the $S(Q)$ $\Delta E$ vs $Q^2$ plot (Fig. 11). The value was significantly higher than that deduced from the dc conductivity (using the Nernst–Einstein equation) and activation energy was lower. Thus, at ambient temperature, $D_n = 9.10^{-7}$ $cm^2$ $S^{-1}$ whereas $D_{\sigma dc} = 10^{-9}$ $cm^2$ $S^{-1}$ and $E_n = 0.15$ eV while $E_{dc} = 0.34$ eV. It is interesting to note that $E_n$ is extremely similar to the $E'_{ac}$ energy deduced from the frequency electrical measurements ($E'_{ac} = 0.14$ eV).

These results are ascribed to the fact that the QENS measurement probe (short range) ionic diffuse motions at high frequencies ($\approx 10^{11}$ Hz); (the characteristic time scale monitored by the time of flight neutron spectrometer used was $10^{-10}$–$10^{-12}$ S).

## Conclusions

The various effects which can be termed "structural" and which affect conductivity in glasses have been illustrated for $Li^+$ and $Ag^+$ ionically conductive chalcogenide glasses. Work concerning their relaxational behavior through a broad frequency range (possible because of the high conductivity of these glasses) was then presented. All the latter results are still preliminary, but a first feature should be stressed. Two activation energies can be deduced in all the materials

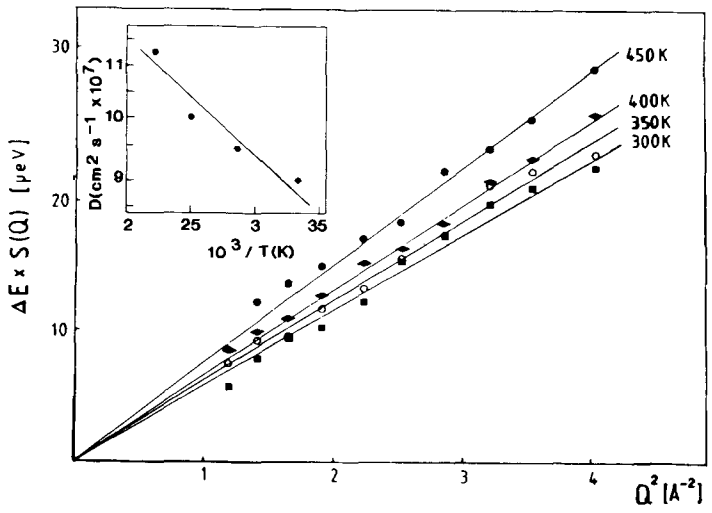


FIG. 11. Plot of the QENS data for 0.5 $Ag_2S$–0.5 $GeS_2$ plotted as $S(Q)\Delta E$ vs $Q^2$. Shown as an inset is the temperature dependence of the $Ag^+$ diffusion coefficient (*29*).

studied and according to the frequency domain investigated. Activation energy $E_{dc}$ is observed at low frequency (mechanical spectroscopy, impedance spectroscopy, high temperature side of the peak of the SLR rate). Lower activation energy $E'$ can be drawn from high frequency measurements (QENS ($E_n$), impedance spectroscopy ($E'_{ac}$), low temperature side of the peak of the SLR rate ($E'_{NMR}$)) placing the relation $E' = \beta E_{dc}$ on a more solid experimental footing.

These results must be completed in the future, in particular by very high frequency electrical measurements in the GHz range and by $^7$Li NMR measurements at frequencies of some 100 MHz to confirm the existence of the two events on the SLR rate curves.

TABLE I

CHARACTERISTICS OF ELECTRICAL CONDUCTIVITIES AND SPIN LATTICE RELAXATION RATES $T_1^{-1}$

| Glass Composition | $E_{dc}$ | $E'_{10kHz}$ | $E'_{100kHz}$ | $E'_{1MHz}$ | $E'_{10MHz}$ | $\langle E'_{ac}\rangle$ | $E_{NMR}$[a] | $E'_{NMR}$[b] | $\beta$[c] | $\beta$[d] | $s$[e] |
|---|---|---|---|---|---|---|---|---|---|---|---|
| 0.5 $Ag_2S$–0.5 $GeS_2$ | 0.34 | 0.15 | 0.14 | 0.14 | 0.13 | 0.14 | — | — | 0.41 | | 0.57 |
| 0.625 (0.5 $Ag_2S$–0.5 $GeS_2$) 0.375 AgI | 0.32 | 0.14 | 0.13 | 0.14 | 0.11 | 0.13 | — | 0.08(10.7) | 0.4 | 0.25 | 0.56 |
| 0.2 $Ag_2Se$–0.8 $GeSe_3$ | 0.34 | 0.16 | 0.16 | 0.15 | 0.13 | 0.15 | — | — | 0.44 | — | 0.66 |
| 0.3 $Li_2S$–0.7 $SiS_2$ | 0.46 | — | — | — | — | — | — | 0.19(15.8) | — | 0.41 | |
| 0.4 $Li_2S$–0.6 $SiS_2$ | 0.37 | 0.17 | 0.15 | 0.16 | 0.13 | 0.15 | — | 0.16(15.8) | 0.41 | — | |
| 0.5 $Li_2S$–0.5 $SiS_2$ | 0.32 | 0.13 | 0.12 | 0.15 | 0.12 | 0.13 | 0.35 | 0.12(15.8) | 0.41 | 0.38 | 0.62 |
| 0.6 $Li_2S$–0.4 $SiS_2$ | 0.32 | — | — | — | — | — | 0.29 | 0.13(15.8) | | 0.4 | |
| 0.56 $Li_2S$–0.44 $SiS_2$ (*32*) | 0.33 | | 0.04 | | | | 0.39 | (0.125)[b] | 0.13 | 0.38 | |

*Note.* Activation energy values are expressed in eV.

[a] $E_{NMR}$ and $E'_{NMR}$ are, respectively, the activation energy of the high and the low temperature sides of the peak of the SLR rate. NMR frequencies in $MH_z$ are given between brackets.

[b] $E'_{NMR}$ has the following values (NMR frequencies in $MH_z$ are given between brackets): 0.134(4), 0.137(7), 0.132(22), and 0.096(40).

[c] $\beta = \langle E'_{ac}\rangle / E_{dc}$.

[d] $\beta = \langle E'_{NMR}\rangle / E_{dc}$.

[e] $s$ is deduced from fitting the experimental curves $\log \sigma'_{ac}$ vs $\log f$ by simplex method.

We have chosen not to discuss the applications of electrolytic glasses here. However, before concluding, several should receive brief mention, since they were often the starting point for much research in solid state ionics. The promising applications for conductive glasses are in two main fields. First, in energy microstorage (*36, 37*) where remarkable results have been obtained by A. Levasseur's team in Bordeaux (*38*) and second, in sensors where thin films of conductive glass are used either in the fabrication of specific electrodes (e.g., the detection of heavy ions (*39*)) or as selective membranes in ISFET (*40*).

## References


1. D. Ravaine and J. L. Souquet, *Phys. Chem. Glasses* **18,** 27 (1977).
2. O. Anderson and P. Stuart, *J. Am. Ceram. Soc.* **37,** 573 (1954).
3. K. L. Ngai, *Comments Solid State Phys.* **9,** 127 (1979); **9,** 141 (1980).
4. K. L. Ngai, A. K. Rajagopal, and S. Teitler, *J. Chem. Phys.*, **88,** 5086 (1988).
5. K. L. Ngai and R. W. Rendell, *Phys. Rev.* **B38,** 9987 (1988).
6. K. Funke, *Solid State Ionics* **18–19,** 183 (1986); **28–30,** 100 (1988).
7. K. Funke and R. Hoppe, *Solid State Ionics* **40–41** 200 (1990).
8. S. R. Elliott, *Solid State Ionics,* **27,** 131 (1988).
9. S. R. Elliott, *Mater. Sci. Eng.* **B3,** 69 (1989).
10. S. R. Elliott and A. P. Owens, *Philos. Mag.* **B60,** 777 (1989).
11. S. R. Elliott and A. P. Owens, *Phys. Rev. B,* **44**(1), 47 (1991).
12. K. Funke and D. Wilmer, *Europhys. Lett.* **12** 363 (1990).
13. G. Balzer-Jöllenbeck, O. Kanert, H. Jain, and K. L. Ngai, *Phys. Rev.* **B39** 6071 (1989).
14. E. Robinel, B. Carette, and M. Ribes, *J. Non-Cryst. Solids* **57,** 49 (1983).
15. A. Pradel and M. Ribes, *Solid State Ionics* **18–19,** 351 (1986).
16. A. Pradel and M. Ribes, *Mat. Chem. Phys.*, **23,** 121 (1989).
17. M. Yoshiyagawa and M. Tomozawa, *J. Phys. Colloque,* **C9,** 411 (1982).
18. V. Michel, A. Pradel, and M. Ribes, *Eur. J. Solid State Inorg. Chem.*, to be published.
19. R. Dupree, D. Holland, and D. S. Williams, *J. Non-Cryst.Solids* **68,** 399 (1984).
20. E. Schneider, J. F. Stebbins, and A. Pines, *J. Non-Cryst. Solids* **89,** 371 (1987).
21. H. Eckert, J. H. Kennedy, A. Pradel, and M. Ribes, *J. Non-Cryst. Solids* **113,** 287 (1989).
22. V. Michel, A. Pradel, M. Ribes, and H. Eckert, *Solid State Ionics,* to be published.
23. V. Deshpande, A. Pradel, and M. Ribes, *Solid State Ionics* **28–30,** 756 (1988).
24. V. Deshpande, A. Pradel, and M. Ribes, *Mater. Res. Bull.* **23,** 379 (1988).
25. A. Pradel, M. Ribes, and M. Maurin, *Solid State Ionics* **28–30,** 762 (1988).
26. J. Ross, D. Brinkmann, M. Mali, A. Pradel, and M. Ribes, *Solid State Ionics* **28–30,** 710 (1988).
27. S. Etienne, J. Perez, A. Pradel, and M. Ribes, *J. Non-Cryst. Solids,* **131–133,** 1072 (1991).
28. A. Pradel and M. Ribes, *J. Non-Cryst. Solids,* **131–133,** 1063 (1991).
29. A. P. Owens, S. R. Elliott, A. Pradel, and M. Ribes, *J. Non-Cryst. Solids,* **131–133,** 1104 (1991).
30. H. Jain and J. N. Mundy, *J. Non-Cryst. Solids* **91,** 315 (1987).
31. S. R. Elliott and F. Henn, *J. Non-Cryst. Solids* **16,** 179 (1990).
32. S. W. Martin, H. K. Patel, F. Borsa, and D. Forgeron, *J. Non-Cryst. Solids,* **131–133,** 1041 (1991).
33. G. Balzer-Jöllenbeck, O. Kanert, J. Steinert, and H. Jain, *Solid State Commun.* **65,** 303 (1988).
34. M. Grüne, H. Meierkord, W. Müller-Warmuth, P. run Hebel, B. Krebs, and M. Wulff, *Ber. Bunsenges, Phys. Chem.* **93** 1313 (1989).
35. A. P. Owens, A. Pradel, M. Ribes, and S. R. Elliott, in "MRS Proceedings, Vol. 210 p. 621 (1991).
36. R. Creus, J. Sarradin, R. Astier, A. Pradel, and M. Ribes, *Mater. Sci. Eng.* **B3** 109 (1989).
37. S. P. Jones, J. R. Akridge, S. G. Humphrey, C. C. Liu, and J. Sarradin, *in* "MRS Proceedings, Vol. 210 p. 31 (1991).
38. A. Levasseur, G. Meunier, R. Dormoy, and M. Menetrier, *in* "Solid State Microbatteries" (J. R. Akridge, and M. Balkanski, eds.), NATO ASI Series, Vol. 217, p. 59 (1990).
39. Y. G. Vlasov and E. A. Bychkov, *in* "Proceedings of the 2nd International meeting on Chemical Sensors, Bordeaux" p. 495, (1986).
40. J. Sarradin, A. Caneiro, P. Fabry, and M. Ribes, *in* "Proceedings of the 3rd International Meeting on Chemical Sensors, Cleveland, Oct. 1990."